DESIGN AND ANALYSIS OF IMPROVED MOUNTAIN GAZELLE OPTIMIZATION TUNED PID AND FOPID CONTROLLERS FOR PV MPPT SYSTEM

By

HEMACHANDRAN VEERASAMY * AROUNASSALAME MOUTTOU ** RATHIDEVI U. ***

*-*** Department of Electrical and Electronics Engineering, Puducherry Technological University, Puducherry, India.

https://doi.org/10.26634/jee.17.4.20985

Date Received: 10/07/2024 Date Revised: 16/07/2024 Date Accepted: 22/07/2024

ABSTRACT

The solar photovoltaic (PV)-based Maximum Power Point Tracking (MPPT) systems have gained popularity in recent times. This work proposes the improvement and implementation of a newly introduced optimization technique, the Improved Mountain Gazelle Optimization (IMGO) algorithm, for tuning the Fractional Order Proportional-Integral-Derivative (FOPID) and Proportional-Integral-Derivative (PID) controllers for the MPPT control strategy. The performances of the controllers were evaluated with reference to error criteria and settling time of the response. The performance parameters mentioned above are compared with those of PID and FOPID controllers tuned using Genetic Algorithm (GA) and Grey-Wolf Optimization (GWO) algorithms. The simulation study was carried out in the MATLAB/SIMULINK environment. The analysis found that the FOPID controller tuned using the Improved Mountain Gazelle Optimization algorithm provides better results in terms of settling time and error when compared to the PID controller.

Keywords: Boost Converter, PID Controller, FOPID Controller, Improved Mountain Gazelle Optimization, Maximum Power Point Tracking.

INTRODUCTION

The development of renewable energy systems for extracting electrical power has recently led to a significant revolution in mitigating the adverse effects of fossil fuels, such as acid rain and global warming. Among the various renewable energy sources, solar photovoltaic (PV) systems are widely implemented in both high- and low-power applications due to their availability, economy, reliability, and controllability. Consequently, the field of power electronics has advanced, as all renewable energy systems rely on power electronic converters. Among these converters, DC-DC converters are especially prominent in applications.

The Maximum Power Point Tracking (MPPT) strategy is used to extract the maximum power from a solar PV system at any given moment. This work focuses on implementing a boost converter for MPPT control, as opposed to a buck converter (Glasner & Appelbaum, 1996). An effective MPPT algorithm is essential for any renewable energy system due to the variable nature of the input. Several MPPT algorithms are available, including Perturb and Observe (P&O), Incremental Conductance (Inc. Cond.), and fuzzy logic-based MPPT (Elgendy et al., 2012; Gupta et al., 2021; Manoharan et al., 2020; Ullah et al., 2023). These algorithms utilize current and voltage data from the PV system to track the Maximum Power Point (MPP) by adjusting the output to match the MPP PV voltage. The controller continuously tracks this MPP PV voltage to ensure optimal power extraction.

Implementing power electronic converters for power transfer in renewable energy systems requires a robust controller to manage the converter's duty ratio, modulation index, carrier frequency, and other parameters. The controller ensures the system's stability and tractability. This work aims to track the Maximum Power Point (MPP) of the solar PV system using a DC-DC boost converter. Typically, Proportional-Integral-Derivative (PID) controllers are used in industrial applications due to their ease of design and implementation, as well as their ability to provide better tracking and stability (Sundareswaran & Sreedevi, 2008). However, PID controllers rely on integral and derivative components, which can lead to issues such as high tracking error, slow settling time, and delayed response to disturbances. To address these issues, Fractional Order PID (FOPID) controllers have been introduced (Adhul & Ananthan, 2020). FOPID controllers use fractional derivatives and integrals, increasing the tuning parameters from three to five, Kp, Ki, Kd, λ, and μ. Although this expansion increases the complexity of the tuning problem, it also enhances flexibility in selecting parameter values.

The increased dimension of the problem calls for better and improved tuning techniques. Many metaheuristic optimization algorithms are implemented for the tuning of the FOPID controller parameters in the literature (Joseph et al., 2022). They are Genetic Algorithm (GA), Particle-Swarm Optimization (PSO) (Afrasyabi et al., 2023), Ant Colony Optimization (ACO) (González et al., 2022), Bee Colony optimization (BCO) (Vanchinathan & Selvaganesan, 2021), Whales Optimization (WO) (Chen et al. 2019), Grey-Wolf Optimization (GWO) (Mirjalili et al. 2014), Golden-Eagle Optimization (GEO) (Mohammadi-Balani et al., 2021), Gorilla Troop Optimization (GTO) (Mostafa et al., 2023), etc. These are commonly used for the designing of controllers as of today. This work proposes an improvement in the Mountain Gazelle Optimization (MGO) algorithm which is a newly developed metaheuristic optimization algorithm introduced in 2022 (Abdollahzadeh et al., 2022). The FOPID controllers are tuned with the IMGO algorithm, and the responses are compared with the FOPID controllers tuned using other generally used optimization algorithms namely the GA and GWO.

Sundareswaran and Sreedevi (2008) have implemented queen bee-assisted GA for designing the PID controller parameters for a boost converter and analyzed its effectiveness by comparing it with the Ziegler- Nichole's Tuning and the standard genetic algorithm tuning (Sundareswaran & Sreedevi, 2008). Later on, as the simulation and implementation of the FOPIDs has become feasible the metaheuristic optimizations have been used for the tuning of the five FOPID controller parameters. Have implemented particle-swarm optimization for the design of a FOPID controller for a cascaded boost converter and analyzed its efficiency with PID controllers (Fernández-Bustamante et al., 2023). The FOPID controllers provide better results than integer-order PID controllers.

By following the trend of controller design for MPPT Fernández-Bustamante et al. (2023) have implemented the sliding mode control for the MPPT control strategy and have compared the results with PID controllers (Shadoul et al. 2017). The use of the FOPID controller provides better performance than the PID controllers in terms of the settling time and the error criteria.

The PID/FOPID controllers tuned using Genetic Algorithms found to be taking much time for convergence and sometimes the result may fall in local minima. The Grey Wolf Optimization algorithm was developed to avoid these drawbacks but the performance of the controller designed using GWO algorithm was not satisfactory.

A need is there for an algorithm which guarantees convergence and performance enhancement. The recently proposed MGO algorithm is promising one due to the characteristics of parallel exploration and exploitation. The convergence is guaranteed and performance improvement is also satisfactory. In this paper an improvement is proposed in the existing MGO to improve the searching capability. The system response of the FOPID controller tuned using the IMGO is compared with the other FOPID and PID controllers tuned using the GA and the GWO and the results are presented.

1. MPPT Concept

The solar PV system converts the solar from the sun's irradiation into usable electrical energy. The power generated from the solar PV system varies as the solar irradiation varies with time, due to sun position, clouds, buildings, etc. Hence the concept of Maximum Power-Point Tracking (MPPT) has been introduced and various techniques have been proposed to extract the maximum power from the PV system available at the specific instance of time, namely the Perturb and Observation (P&O) (Manoharan et al. 2020), Incremental Conductance (Inc. Cond.) (Gupta et al., 2021), fuzzy logic-based MPPT (Ullah et al., 2023), curve-fitting technique (Abdollahzadeh et al., 2022), etc. These MPPT techniques sense the PV voltage (V_{pv}) and current (I_{pv}) of past and current values and give the Maximum Power Point (MPP) voltage (V*) or MPP duty ratio of the converter. This paper implements the strategy of providing MPP voltage and the controller is implemented to sense the error produced from the difference between the PV voltage and the MPP voltage, and provide the duty ratio, and the pulses are generated for the DC-DC boost converter. The diagram of the system is shown in Figure 1.

2. MPPT Technique

The MPPT technique used in this work is the Incremental Conductance (Inc. Cond.) technique (Gupta et al., 2021). It is evident that at the MPP the slope dP_s/dV_s is zero. This Inc. Cond. technique uses this condition to track the MPP which has a slope of zero. The governing conditions for the Inc. Cond. technique are given in (1) - (3).

$$P_S = V_S \times I_S \tag{1}$$

$$\frac{1}{V_S} \times \frac{dP_S}{dV_S} = \frac{I_S}{V_S} + \frac{dI_S}{dV_S} \tag{2}$$

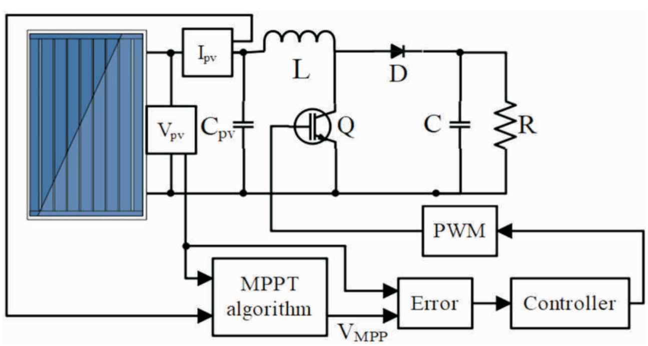

Figure 1. Schematic Diagram of the MPPT-based Boost Converter for the PV System

$$\left\{ \begin{array}{l} \frac{dP_S}{dV_S} = 0, if \ \frac{dI_S}{dV_S} = \frac{I_S}{V_S} (at\ MPP) \\ \frac{dP_S}{dV_S} > 0, if \ \frac{dI_S}{dV_S} > \frac{-I_S}{V_S} (left\ of\ MPP) \\ \frac{dP_S}{dV_S} < 0, if \ \frac{dI_S}{dV_S} < \frac{-I_S}{V_S} (right\ of\ MPP) \end{array} \right\} \tag{3}$$

3. Boost Converter

The DC-DC boost converter is mathematically modeled. The DC-DC boost converter is a power electronic circuit that converts the solar PV DC voltage, V_s which is the input to the converter into the variable output DC voltage, V_{out} higher than the input DC voltage. The boost converter is made of various components namely, a diode, a capacitor, an inductor, a load, and a power electronic switch. The boost converter varies the output DC voltage by varying the duty ratio, d_p of the switching pulses to the power electronic switch. The output voltage equation of the boost converter is presented in (4).

$$V_{out} = V_S \frac{1}{(1-d_p)} \tag{4}$$

where duty cycle, d_p for on time of the switch in a cycle, T_{on} and the total time of a cycle, T is given by (5).

$$d_p = \frac{T_{on}}{T} \tag{5}$$

The general schematic representation of a boost converter is presented in Figure 2. The equivalent circuit of the boost converter for the conditions of the power electronic switch on and off is applied with Kirchhoff's voltage and Kirchhoff's current laws and the state space model for on and off state is given in (6) – (7) respectively.

$$\begin{bmatrix} \frac{di_L}{dt} \\ \frac{dv_C}{dt} \end{bmatrix} = \begin{bmatrix} 0 & -\frac{1}{L_b} \\ \frac{1}{C_b} & -\frac{1}{RC_b} \end{bmatrix} \begin{bmatrix} i_L \\ V_C \end{bmatrix} + \begin{bmatrix} \frac{1}{L_b} \\ 0 \end{bmatrix} V_S \tag{6}$$

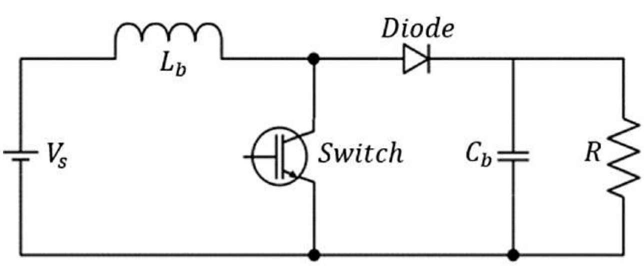

Figure 2. The DC-DC Boost Converter Circuit Diagram

$$\begin{bmatrix} \frac{di_L}{dt} \\ \frac{dv_C}{dt} \end{bmatrix} = \begin{bmatrix} 0 & 0 \\ 0 & -\frac{1}{RC_b} \end{bmatrix} \begin{bmatrix} i_L \\ V_C \end{bmatrix} + \begin{bmatrix} \frac{1}{L_b} \\ 0 \end{bmatrix} V_S \quad (7)$$

Where, i_L, v_C, L_b, C_b, V_S and R are inductor current, capacitor voltage, inductor, capacitor, solar PV voltage, and load resistor respectively. The above state space models are used to obtain the average state space model for the boost converter given in (8) and (9).

$$\begin{bmatrix} \frac{di_L}{dt} \\ \frac{dv_C}{dt} \end{bmatrix} = \begin{bmatrix} 0 & -\frac{(1-d_p)}{L_b} \\ \frac{(1-d_p)}{C_b} & -\frac{1}{RC_b} \end{bmatrix} \begin{bmatrix} i_L \\ V_C \end{bmatrix} + \begin{bmatrix} \frac{1}{L_b} \\ 0 \end{bmatrix} V_S \quad (8)$$

$$V_{out} = [0 \quad 1] \begin{bmatrix} i_L \\ v_C \end{bmatrix} \quad (9)$$

For designing the PID and FOPID controllers the small signal transfer function model is derived using the perturbation and linearization technique. The converter parameters could be expressed as follows in the presence of a small perturbation and given in (10).

$$\begin{aligned} i_L &= I_L + \tilde{i}_L \\ v_c &= V_c + \tilde{v}_c \\ V_s &= V_s + \tilde{v}_s \\ V_{out} &= V_{out} + \tilde{v}_{out} \\ d_p &= D_p + \tilde{d}_p \end{aligned} \quad (10)$$

Substituting these in the average state space model (8) – (9) and the small signal state space model is presented in (11) and (12).

$$\begin{bmatrix} \frac{d\tilde{i}_L}{dt} \\ \frac{d\tilde{v}_C}{dt} \end{bmatrix} = \begin{bmatrix} 0 & -\frac{(1-D_p)}{L_b} \\ \frac{(1-D_p)}{C_b} & -\frac{1}{RC_b} \end{bmatrix} \begin{bmatrix} i_L \\ V_C \end{bmatrix} + \begin{bmatrix} \frac{1}{L_b} & \frac{V_{out}}{L_b} \\ 0 & -\frac{I_L}{C_b} \end{bmatrix} \begin{bmatrix} v_S \\ d_p \end{bmatrix} \quad (11)$$

$$\tilde{v}_{out} = [0 \quad 1] \begin{bmatrix} \tilde{i}_L \\ \tilde{v}_C \end{bmatrix} \quad (12)$$

This small signal state space model (11) – (12) is used to obtain a small signal transfer function given in (13). The obtained transfer function model is simplified using the small signal duty ratio equation and the final small signal transfer function model, v_s/d_p which is given in (14) and is used for the designing of PID and FOPID controllers.

$$\frac{v_{out}}{d_p} = \frac{(1-D_p)V_{out} - (L_b I_L)s}{L_b C_b s^2 + \frac{L_b}{R}s + (1-D_p)^2} \quad (13)$$

$$\frac{v_s}{d_p} = \frac{(1-D_p)^2 V_{out} - (1-D_p)(L_b I_L)s}{L_b C_b s^2 + \frac{L_b}{R}s + (1-D_p)^2} \quad (14)$$

4. Improved Mountain Gazelle Optimization

4.1 Mountain Gazelle Optimizer

Mountain Gazelle Optimization (MGO) is a newly introduced metaheuristic optimization algorithm for multi- dimensional and multi-objective optimization problems (Abdollahzadeh et al., 2022). This optimization algorithm mimics the social behavior of the mountain gazelle. They are highly territorial, and they travel to distant places for migration. The algorithm uses the following four behaviors to model the behavior of the mountain gazelles, namely the territorial solitary male, the maternity herd, the bachelor male herd, and the migration for food search. These four methodologies generate new solutions in parallel and they are added to the population. In the first process, the Territorial Solitary Male (TSM) imitates the behavior of the adult male gazelle. Adult male gazelle is highly territorial and the process of trying to protect the territory and the procession of females is modeled in (15).

$$TSM = m_g - |(rin_1 \times B - rin_2 \times X) \times f| \times C_r \quad (15)$$

Where, rin_1 and rin_2 take values randomly either 1 or 2, X is the current solution vector (gazelle), m_g is the adult male gazelle which is the best solution in the current iteration, B is the coefficient of young males which is calculated each time using (16).

$$B = X_{ra} \times [rr_1] + M_{pr} \times [rr_2] \quad (16)$$

Where rr_1 and rr_2 are randomly generated real numbers between the range 0 and 1, M_{pr} is the average of the randomly selected [N/3] gazelles (solutions), N is the total population count, and X_{ra} is the solution randomly selected from the range of [N/3] to N which selects from [2N/3] gazelles. The value of f is given by (17).

$$f = n_1 \times e^{\left(2 - Iter \times \left(\frac{2}{MaxIter}\right)\right)} \quad (17)$$

Where n_1 takes a random value of the dimension in the standard distribution, Iter and MaxIter is the present iteration count and the maximum iteration count respectively. C_r is the convergence coefficient selected randomly which is given by (18).

$$C_r = \begin{Bmatrix} (A+1)+rr_3 \\ A \times n_2 \\ rr_4 \\ n_3 \times n_4{}^2 \times \cos((rr_5 \times 2) \times n_3) \end{Bmatrix} \quad (18)$$

Where n_2, n_3 and n_4 takes a random value of problem dimension in the standard distribution, rr_3, rr_4 and rr_5 are random real numbers between 0 and 1, and the value of A is given by (19).

$$A = -1 + Iter \times \left(\frac{-1}{MaxIter} \right) \quad (19)$$

The Maternity Herd (MH) is responsible for the birth of new young male gazelles and their parenting. In this behaviour both the adult male and young males also play a role. This behavior is mathematically modeled in (20).

$$MH = (B + C_r) + (rin_3 \times m_g - rin_4 \times X_{ran}) \times C_r \quad (20)$$

Where rin_3 and rin_4 takes the values either 1 or 2 randomly and X_{ran} is a randomly selected gazelle from the total population. The Bachelor Male Herd (BMH) models the behavior of young males who are mature to a certain level. These mature young male gazelles are involved in the fights for new territory creation and female procession and this model is given in (21).

$$BMH = (X - Da) + (rin_5 \times m_g - rin_6 \times B) \times C_r \quad (21)$$

Where rin_5 and rin_6 takes the values either 1 or 2 randomly and the value of Da is presented in (22).

$$Da = \left(|X| + |m_g| \right) \times (2 \times rr_5 - 1) \quad (22)$$

Where rr_5 takes the random real numbers between 0 and 1. The Migration for Food Search (MFS) is the last behavior modeled in (23). The gazelles travel a long distance in search of food and shelter.

$$MFS = (u\text{-}l) \times rr_6 + l \quad (23)$$

Where u and l are the upper bounds and the lower bounds of the solutions, and rr_6 is a random real number between 1 and 0 which is a real value. The new solutions (gazelles) generated in each iteration are added to the gazelle population, the best N gazelles are retained, and the worst solutions are eliminated from the gazelle population. The flowchart of the MGO is presented in Figure 3.

4.2 Proposed Improvement

In the Mountain Gazelle Algorithm (MGO), the equation for young male herd coefficient given in (16) the floor and ceil functions are implemented for random values rr_1 & rr_2 respectively. Since the random values are in the range of 0 to 1, this forces the participation factor of X_{ra} and M_{pr} to 0 and 1 irrespective of the random values of rr_1 & rr_2. So, the above floor and ceil functions are replaced with a round-off function so that the participation factor of X_{ra} and M_{pr} is varied for each iteration which is given in (24).

$$B = X_{ra} \times [rr_1] + M_{pr} \times [rr_2] \quad (24)$$

Here the values of rr_1 & rr_2 can take values 0 & 0, 0 &1, 1 & 0 and, 1 & 1. This modification will improve the searching space. The Improved MGO is used for the designing of FOPID and PID controllers with the objective function of reducing the Integral Time Weighted Square Error (ITWSE).

5. Controller Design

The error sensed by the controllers between the solar PV

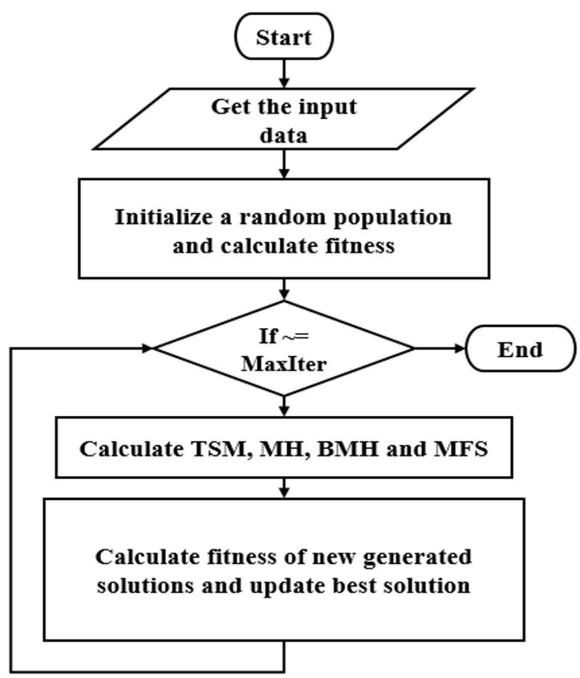

Figure 3. Flowchart of Mountain Gazelle Optimization Algorithm

voltage, V_s, and the MPP voltage, V* is reduced by the use of control action. This section presents the design of various controllers for MPPT. The error signal used in the control strategy is given in (25).

$$e = V_s - V^* \quad (25)$$

5.1 PID Controller

The PID controller is a commonly used controller due to its simplicity and ease of control and design. The PID controller takes the error as input and performs proportional action, integral action, and derivative action and outputs the control signal to the pulse generator and in turn to the switch of the boost converter. The PID controller is defined in (26).

$$G_{PID}(s) = K_p + \frac{K_i}{s} + K_d s \quad (26)$$

The main objective for designing the PID controller is the selection of proportional constant K_p, integral constant K_i, and derivative constant K_d. This is important to ensure better performance of the PID controller. There are various tuning methods for the selection of the PID gains namely the classical Ziegler Nichole's tuning, metaheuristic optimization algorithm tuning, etc. This paper implements Genetic Algorithm (GA), Grey-Wolf Optimization (GWO), and Improved Mountain Gazelle Optimization (IMGO) for the tuning of the PID gains.

5.2 FOPID Controller

Due to the limitations in expressing the real-time systems in integer-order derivatives, the Fractional Order (FO) calculus has been introduced. This concept has been introduced in PID controllers too, naming them Fractional Order PID (FOPID) controllers. The FOPID control Fernández-Bustamante et al. (2023) is defined in (27). The FOPID controller is identified to perform better when compared to the integer-order PID controllers in terms of fast system response, low settling time, etc.

$$G_{F0PID}(s) = K_p + \frac{K_i}{s^{\lambda}} + K_d s^{\mu} \quad (27)$$

Here the complexity of the tuning is higher due to the presence of additional terms, namely the order of fractional integral, λ, and the order of fractional derivative, μ. Generally, one could choose the range of λ and μ in a range of real numbers between 0 and 2. Hence the problem becomes five dimensional. So, a better metaheuristic optimization technique is necessary. This work implements GA, GWO, and IMGO for the design of FOPID controller parameters.

6. Simulation Results

The system is implemented and analyzed in the MATLAB/SIMULINK platform. Table 1 shows the specification details of the DC-DC boost converter that is implemented. The specifications for the 1kW solar PV panel implemented are shown in Table 2. The transfer function for the boost converter is obtained from (14) and it aids in the designing of PID and FOPID controller constants and is presented in (28). The simulation is carried out for the duration of 1 second with the step disturbance at 0.5 seconds from 500 to 1000 W/m^2 irradiance.

$$\frac{v_s}{d_p} = \frac{30 - 0.0075s}{(6.25\times10^{-8})s^2 + (6.25\times10^{-5})s + 0.25} \quad (28)$$

The parameters used for the metaheuristic optimization algorithms used for the designing of PID and FOPID controllers, namely the GA, GWO and the Improved MGO are shown in Table 3.

The PID controller gains obtained with the help of metaheuristic optimization techniques are presented in Table 4. These PID controllers are implemented in the DC-DC boost converter system for MPPT. The performance parameters namely the Integral Time Weighted Square

Parameters	Values	Units
Input Voltage (V_{in})	60	V
Output Voltage (V_o)	120	V
Capacitor Value (C)	10	μF
Inductor Value (L)	6.25	mH
Switch Switching Frequency (f_s)	25	kHz
Load Resistor (R)	100	Ω

Table 1. Boost Converter Specifications

Array Data		
Parameters	Values	Units
Parallel Strings	2	Numbers
Series Connected Modules Perstring	2	Numbers
Module – 1Soltech 1STH-250_WH		
Maximum PV Power (W)	250.205	W
Cells/Module (N_{cell})	60	Numbers
Short Circuit Current (I_{sc})	8.66	A
Open Circuit Voltage (V_{oc})	37.3	V
MPP Current (I_{mp})	8.15	A
MPP Voltage (V_{mp})	30.7	V

Table 2. Solar PV Array Specifications

Error (ITWSE) and the setting time of the response are presented in Table 5 where it is inferred that the PID controller designed using the Improved MGO algorithm performs better than GWO and GA. The output response graphs for the system are shown in Figure 4 and 5.

The FOPID controller parameters tuned using the metaheuristic algorithms are shown in Table 6. The system response parameters, namely the ITWSE and settling time are shown in Table 7. The output response graphs are shown in Figure 6 and 7. From the results it is inferred that the FOPID controller designed using the Improved MGO outperforms other FOPID controllers designed using GWO and GA.

Parameters	Values
Size of Population (N_p)	30
Iteration Count (Iter)	10
Crossover Distribution Index (etac)	20
Mutation Distribution Index (etam)	20
Crossover Probability (P_c)	0.8
Mutation Probability (P_m)	0.2

Table 3. Optimization Algorithm Parameters

Optimization Techniques	K_p	K_i	K_d
Genetic Algorithm	0.0001	2.0194	0
Grey Wolf Optimization	0.0018	4.0181	0
Improved Mountain Gazelle Optimization	0.00195	4.3605	1×10^{-6}

Table 4. Optimization Algorithm Results for PID Controller Parameters

Optimization Techniques	Integral Time- Weighted Square Error	Setting Time (s)
Genetic algorithm	0.003618	0.05
Grey wolf optimization	0.001917	0.016
Improved mountain gazelle optimization	0.001791	0.015

Table 5. Performance Comparison of the System using PID Controllers

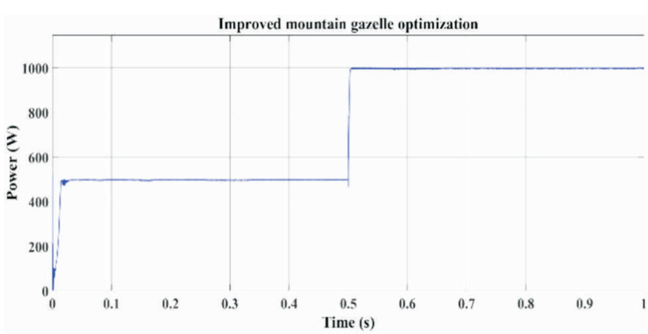

Figure 4. Closed Loop System Response with PID Tuned using IMGO

The overall comparison of the PID controller tuned using the IMGO, and the FOPID controller tuned using the IMGO which have provided the best result among the PIDs, and FOPIDs are presented in Table 8. The closed loop system response comparison by implementing the above various control methodologies is presented in Figure 8. From these results it is inferred that the FOPID controller designed using IMGO performs better than other controllers.

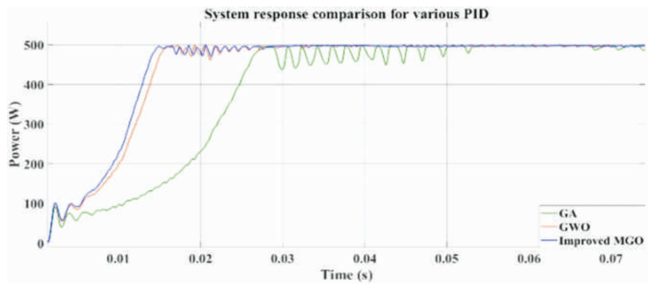

Figure 5. Closed Loop System Response using Various PID Controllers

Optimization Techniques	K_p	K_i	λ	K_d	μ
Genetic Algorithm	0.0036	5.069	0.940	0	0
Grey Wolf Optimization	0.0031	4.787	0.910	0	0
Improved Mountain Gazelle Optimization	0.01	6.313	0.899	1×10^{-6}	1.19

Table 6. Optimization Algorithm Results for FOPID Controller Parameters

Optimization Techniques	Integral Time- Weighted Square Error	Setting Time (s)
Genetic algorithm	0.001182	0.0101
Grey wolf optimization	0.001101	0.0093
Improved mountain gazelle optimization	0.0007091	0.007

Table 7. Performance Comparison of the System using FOPID Controllers

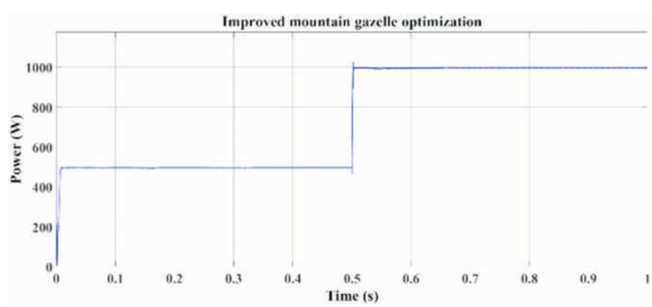

Figure 6. Closed Loop System Response with FOPID Tuned using IMGO

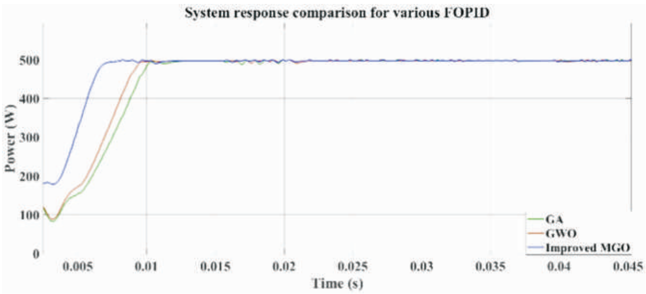

Figure 7. Closed Loop System Response using Various FOPID Controllers

Optimization Techniques	Integral Time- Weighted Square Error	Setting Time (s)
PID controller tuned using Improved MGO	0.001791	0.015
FOPID controller tuned using Improved MGO	0.0007091	0.007

Table 8. Performance Comparison of the System using Various Controllers

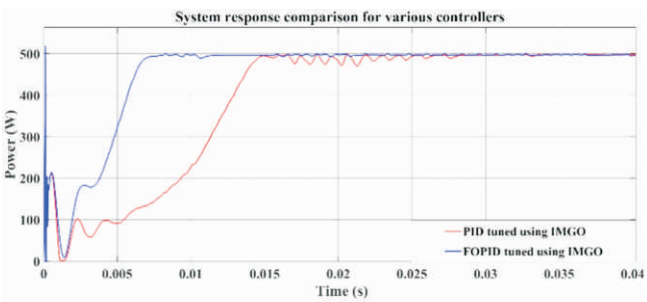

Figure 8. Closed Loop System Response using Various Controllers

Conclusion

This paper implements PID and FOPID control methods for MPPT in PV-based DC-DC boost converters. The PID controller and the FOPID controller are tuned using theImproved Mountain Gazelle Optimization algorithm and the performance is compared with other controllers tuning using the GA and the GWO. The IMGO algorithm is found to be better than other metaheuristic optimization techniques due to its methodology of exploration and exploitation carried out in parallel. The simulation analysis is performed in the MATLAB/SIMULINK platform. From the obtained results, the FOPID controller tuned using IMGO provides better performance in terms of setting time and also has a considerably lower ITWSE than the PID controller tuned using IMGO. The MPPT is implemented in high-power solar applications and as in real-time, the solar irradiation varies with respect to time, preventing the system from attaining a steady state. The FOPID controller tuned using the IMGO provides a better response; hence, this controller can be implemented in the MPPT-based solar PV system. The implementation of the hardware model for the fractional integrators and differentiators involves much complex circuits. The hardware implementation is not carried out in this paper. But much research works is progressing in this area.

References

[1]. **Abdollahzadeh, B., Gharehchopogh, F. S., Khodadadi, N., & Mirjalili, S. (2022).** Mountain gazelle optimizer: A new nature-inspired metaheuristic algorithm for global optimization problems. *Advances in Engineering Software*, 174, 103282.

https://doi.org/10.1016/j.advengsoft.2022.103282

[2]. **Adhul, S. V., & Ananthan, T. (2020).** FOPID controller for buck converter. *Procedia Computer Science*, 171, 576-582.

https://doi.org/10.1016/j.procs.2020.04.062

[3]. **Afrasyabi, P., Mesgari, M. S., El-sayed, M., Kaveh, M., Ibrahim, A., & Khodadadi, N. (2023).** A crossover-based multi-objective discrete particle swarm optimization model for solving multi-modal routing problems. *Decision Analytics Journal*, 9, 100356.

https://doi.org/10.1016/j.dajour.2023.100356

[4]. **Chen, H., Xu, Y., Wang, M., & Zhao, X. (2019).** A balanced whale optimization algorithm for constrained engineering design problems. *Applied Mathematical Modelling*, 71, 45-59.

https://doi.org/10.1016/j.apm.2019.02.004

[5]. **Elgendy, M. A., Zahawi, B., & Atkinson, D. J. (2012).** Assessment of the incremental conductance maximum power point tracking algorithm. *IEEE Transactions on Sustainable Energy*, 4(1), 108-117.

https://doi.org/10.1109/TSTE.2012.2202698

[6]. **Fernández-Bustamante, P., Calvo, I., Villar, E., & Barambones, O. (2023).** Centralized MPPT based on sliding mode control and XBee 900 MHz for PV systems.

International Journal of Electrical Power & Energy Systems, 153, 109350.

https://doi.org/10.1016/j.ijepes.2023.109350

[7]. Glasner, I., & Appelbaum, J. (1996, November). Advantage of boost vs. buck topology for maximum power point tracker in photovoltaic systems. In *Proceedings of 19th Convention of Electrical and Electronics Engineers in Israel* (pp. 355-358). IEEE.

https://doi.org/10.1109/EEIS.1996.566988

[8]. González, P., Prado-Rodriguez, R., Gábor, A., Saez-Rodriguez, J., Banga, J. R., & Doallo, R. (2022). Parallel ant colony optimization for the training of cell signaling networks. *Expert Systems with Applications*, 208, 118199.

https://doi.org/10.1016/j.eswa.2022.118199

[9]. Gupta, A. K., Pachauri, R. K., Maity, T., Chauhan, Y. K., Mahela, O. P., Khan, B., & Gupta, P. K. (2021). Effect of various incremental conductance MPPT methods on the charging of battery load feed by solar panel. *IEEE Access*, 9, 90977-90988.

https://doi.org/10.1109/ACCESS.2021.3091502

[10]. Joseph, S. B., Dada, E. G., Abidemi, A., Oyewola, D. O., & Khammas, B. M. (2022). Metaheuristic algorithms for PID controller parameters tuning: Review, approaches and open problems. *Heliyon*, 8(5), E09399.

https://doi.org/10.1016/j.heliyon.2022.e09399

[11]. Manoharan, P., Subramaniam, U., Babu, T. S., Padmanaban, S., Holm-Nielsen, J. B., Mitolo, M., & Ravichandran, S. (2020). Improved perturb and observation maximum power point tracking technique for solar photovoltaic power generation systems. *IEEE Systems Journal*, 15(2), 3024-3035.

https://doi.org/10.1109/JSYST.2020.3003255

[12]. Mirjalili, S., Mirjalili, S. M., & Lewis, A. (2014). Grey wolf optimizer. *Advances in Engineering Software*, 69, 46-61.

https://doi.org/10.1016/j.advengsoft.2013.12.007

[13]. Mohammadi-Balani, A., Nayeri, M. D., Azar, A., & Taghizadeh-Yazdi, M. (2021). Golden eagle optimizer: A nature-inspired metaheuristic algorithm. *Computers & Industrial Engineering*, 152, 107050.

https://doi.org/10.1016/j.cie.2020.107050

[14]. Mostafa, R. R., Gaheen, M. A., Abd ElAziz, M., Al-Betar, M. A., & Ewees, A. A. (2023). An improved gorilla troops optimizer for global optimization problems and feature selection. *Knowledge-Based Systems*, 269, 110462.

https://doi.org/10.1016/j.knosys.2023.110462

[15]. Shadoul, M., Al Abri, R., Yousef, H., & Masoud, M. (2017, May). Dc-dc boost converter controller design for pv applications. In 2017 9th *IEEE-GCC Conference and Exhibition (GCCCE)* (pp. 1-6). IEEE.

https://doi.org/10.1109/IEEEGCC.2017.8448164

[16]. Sundareswaran, K., & Sreedevi, V. T. (2008). Boost converter controller design using queen-bee-assisted GA. *IEEE Transactions on Industrial Electronics*, 56(3), 778-783.

https://doi.org/10.1109/TIE.2008.2006026

[17]. Ullah, K., Ishaq, M., Tchier, F., Ahmad, H., & Ahmad, Z. (2023). Fuzzy-based maximum power point tracking (MPPT) control system for photovoltaic power generation system. *Results in Engineering*, 20, 101466.

https://doi.org/10.1016/j.rineng.2023.101466

[18]. Vanchinathan, K., & Selvaganesan, N. (2021). Adaptive fractional order PID controller tuning for brushless DC motor using artificial bee colony algorithm. *Results in Control and Optimization*, 4, 100032.

https://doi.org/10.1016/j.rico.2021.100032

ABOUT THE AUTHORS

Hemachandran Veerasamy is pursuing a B.Tech. in the Department of Electrical and Electronics Engineering at Puducherry Technological University, Puducherry, India. His areas of interest are DC-DC Boost Converters, PID Controllers, FOPID Controllers and Sliding Mode Control.

Dr. Arounassalame Mouttou is working as a Professor in the Department of Electrical and Electronics Engineering at Puducherry Technological University, Puducherry, India. He received his B.Tech. degree from Pondicherry University, India, in 1993 and his M.Tech. degree from the University of Calicut, India, in 1998. He received the Ph.D. degree in Systems and Control Engineering from IIT Bombay, India, in 2009. His areas of interest are High-Gain DC-DC Converters, Control Applications in Power Electronics, and Optimization.

Rathidevi U. is pursuing a B.Tech. in the Department of Electrical and Electronics Engineering at Puducherry Technological University, Puducherry, India. Her areas of interest are DC-DC Boost Converters, PID Controllers and FOPID Controllers.